

Richardson's pair diffusion and the stagnation point structure of turbulence

J. Dávila^{1,*} and J.C. Vassilicos²

¹*E. Superior de Ingenieros, Camino de los Descubrimientos s/n, 41092 - Sevilla, Spain*

²*Department of Aeronautics, Imperial College, London SW7 2BY, UK*

(Dated: November 2, 2018)

DNS and laboratory experiments show that the spatial distribution of straining stagnation points in homogeneous isotropic 3D turbulence has a fractal structure with dimension $D_s = 2$. In Kinematic Simulations the time exponent γ in Richardson's law and the fractal dimension D_s are related by $\gamma = 6/D_s$. The Richardson constant is found to be an increasing function of the number of straining stagnation points in agreement with pair diffusion occurring in bursts when pairs meet such points in the flow.

Keywords: Particle dispersion, homogeneous turbulence

The rate with which pairs of points separate in phase space or in physical space is of central importance to the study of dynamical systems. Pairs of points in the phase space of a low-dimensional chaotic dynamical system separate exponentially. In chaotic advection pairs also separate exponentially [1] leading to exponentially fast stirring and a high potential for mixing. In turbulent flows, however, pairs of fluid elements separate on average algebraically [2, 3, 4]. Turbulent flows have a very wide range of excited length- and time-scales and are therefore fundamentally different from both low-dimensional dynamical systems and chaotic advection flows. Attempts have been made to model the relative diffusion of fluid element pairs in terms of Langevin type equations based on the assumption that relative Lagrangian accelerations are Markovian in time [5, 6]. These models can reproduce the right algebraic time growth of separation statistics of fluid elements in turbulent flows; but they fail to explain the very large values taken by the flatness factor of Lagrangian relative velocities in Direct Numerical Simulations of isotropic turbulence [6, 7, 8]. In fact these models based on Markovian acceleration statistics underestimate this flatness factor by as much as one order of magnitude.

The algebraic growth of Lagrangian separation statistics can also be accurately reproduced by Kinematic Simulations [9, 10, 11]. These are models of turbulent diffusion based on kinematically simulated turbulent velocity fields which are non-Markovian (not delta-correlated in time), incompressible and consistent with up to second order statistics of the turbulence such as energy spectra. Kinematic Simulations are interesting in particular because they do reproduce the very high flatness factors of Lagrangian relative velocities [8]. The mechanism by which fluid element pairs separate in Kinematic Simulations (KS) might therefore be comparable to the one in turbulent flows and is clearly different from the Wiener process which causes fluid element pairs to separate in Lagrangian models of relative diffusion based on Langevin type equations. But what is this mechanism and why can it give rise to the algebraic growth of rela-

tive separations?

Richardson's law of turbulent relative diffusion states that the mean square distance between two fluid elements $\overline{\Delta^2}$ is proportional to the third power of time t , i.e.

$$\overline{\Delta^2}(t) \approx GL^2 \left(\frac{tu'}{L} \right)^\gamma, \quad (1)$$

where $\gamma = 3$, G is a universal dimensionless constant and L and u' are the integral length-scale and the rms velocity of the turbulence respectively. Richardson's law is expected to be valid in homogeneous isotropic turbulence and for times t such that $\overline{\Delta^2}$ is within the inertial range of scales, i.e. $\eta^2 \ll \overline{\Delta^2} \ll L^2$, where η is the Kolmogorov microscale. Fluid element pairs follow close trajectories for long stretches of time and separate violently when they meet straining flow regions around stagnation points (straining stagnation points) [9, 11, 12, 13]. [8] noted that the very high flatness factors of Lagrangian relative velocities are consistent with this conjecture.

[11] found evidence of a fractal spatial distribution of straining flow regions in KS homogeneous isotropic turbulent velocity fields. In this paper we quantify their observation by showing that the number of straining stagnation points per unit volume in KS, Direct Numerical Simulations (DNS) and laboratory experiments of homogeneous isotropic turbulence is given by

$$n_s \approx C_s L^{-3} \left(\frac{L}{\eta} \right)^{D_s} \quad (2)$$

where $D_s = 2$ and C_s is a dimensionless number. The exponent D_s can be interpreted as a fractal dimension. Both (1) and (2) hold for $L/\eta \gg 1$.

We now describe the DNS and the grid turbulence measurements used to establish (2) with $D_s=2$. We have used DNS data of non-decaying homogeneous isotropic incompressible turbulence generated by a standard pseudo-spectral code with grid resolution of about 2η and have computed the number of stagnation points in instantaneous velocity fields $\mathbf{u} = \mathbf{u}(\mathbf{x}) = (u(\mathbf{x}), v(\mathbf{x}), w(\mathbf{x}))$ for a variety of Taylor microscale Reynolds numbers Re_λ ranging from 34 to 130. In this paper we focus our interest on

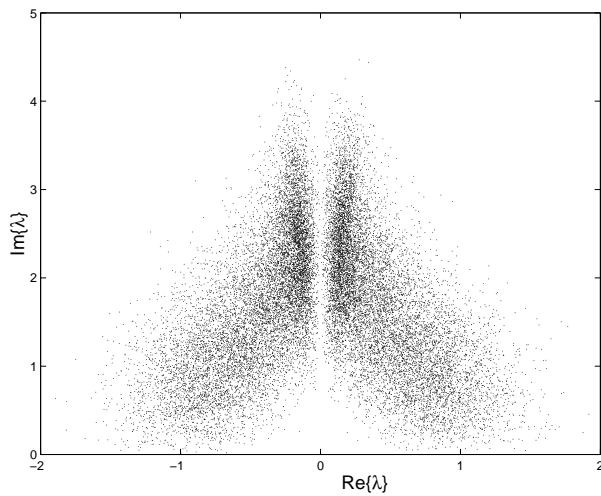


FIG. 1: Imaginary versus real part of the complex eigenvalues of the gradient of velocity matrix with positive imaginary part for 26726 stagnation points in a KS field with $L/\eta \approx 45$. Very few complex eigenvalues with small (absolute) real part can be found. Similar results (with poorer resolutions) were obtained with DNS for similar values of L/η .

the straining flow regions around stagnation points of \mathbf{u} . A stagnation point does indeed correspond to a straining flow region when the eigenvalues of the velocity gradient matrix at this point are all non-zero (see Ottino 1989); these are regions where the flow is always straining and may or may not be rotating as well.

We use the Newton-Raphson method (tested against the amoeba method in various planar flows) to find all stagnation points [14]. This is an iterative method and requires starting points, which have been taken all over the DNS field at points separated by a distance smaller than η . Irrespective of Reynolds number, the vast majority of stagnation points have turned out to be in straining regions. Figure 1 is a scatter plot of the complex eigenvalues of the gradient of velocity matrix. Notice that the probability to find eigenvalues with imaginary part much larger than the real part is very low. The only case where stagnation points can be non-straining is when two eigenvalues are pure imaginary and the third eigenvalue is zero. Hence the number of stagnation points is therefore effectively the same as that of straining stagnation points, and this number per unit volume is n_s . For every Reynolds number, we calculate n_s , L and η and we plot n_s as a function of L/η (see figure 2). The relation between these two quantities appears to be well fitted by (2) with $D_s = 2$.

Experimental support for (2) with $D_s = 2$ has been obtained from grid generated turbulence in the laboratory. The turbulence is homogeneous and isotropic far enough from the grid and from the wind tunnel walls. Measurements of the streamwise air velocity u were taken with a hot wire at the centre of the working section of a wind

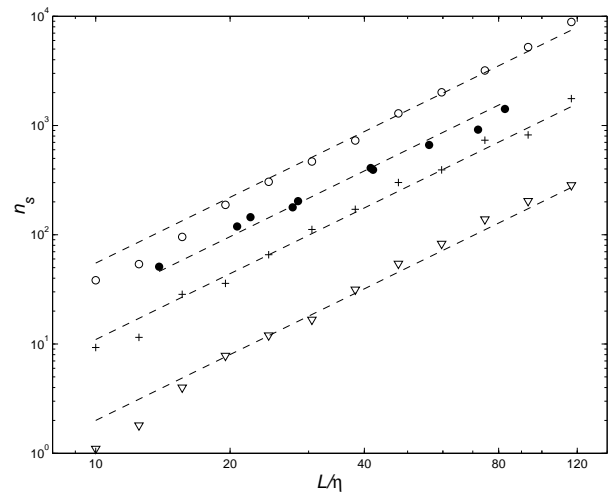


FIG. 2: Number of stagnation points per unit volume versus L/η in DNS (\bullet) and KS for $p = 5/3$ and different values of V (compared to $u' = 1$): \circ $V = 0$, $+$ $V = 0.7$, ∇ $V = 1.0$. Dashed lines representing $n_s \propto (L/\eta)^2$ are shown for comparison.

tunnel at a distance of 50 mesh sizes behind the grid. We collected thirty runs of data for thirty different values of Re_λ ranging from 68 to 130. The sampling frequency was 30 kHz, enough to resolve the dissipation range except at the highest values of Re_λ but always enough, however, to resolve the Taylor microscale in all our runs. Each data set contains more than 100 integral scales. The turbulence intensity was always smaller than 5% thus allowing the use of the Taylor hypothesis for the conversion of temporal data into spatial data. It is possible, from these wind tunnel data, to calculate the number of zero-crossings of u per unit length which leaves us with the problem of relating this number to the number of stagnation points per unit volume in homogeneous and isotropic turbulence. Each component of \mathbf{u} has an instantaneous zero-crossing surface in the three-dimensional space of the flow. These three instantaneous surfaces may have a fractal dimension larger than or equal to 2. Because of isotropy, these three fractal dimensions must be the same and we denote them by D . Stagnation points of \mathbf{u} are intersections of the three zero-crossing surfaces. The rule of the thumb for estimating the fractal dimension of intersections of surfaces is that the codimension is equal to the sum of the codimensions of the intersecting surfaces [15]. The codimension of each zero-crossing surface is $D - 2$ because surfaces are two-dimensional and the codimension of the set of their intersections is $D_s - 0$ because points are zero-dimensional. Hence, $D_s = 3(D - 2)$. We are assuming our DNS observation that the vast majority of stagnation points lie in straining regions to be also true in grid generated turbulence which is why we use the notation D_s for the fractal dimension of the stagnation points of \mathbf{u} .

By virtue of the Taylor hypothesis, the zero-crossings

of our one-dimensional u data can be viewed as a set of point intersections through the zero-crossing surface $u(\mathbf{x}) = 0$. From our one-dimensional data the codimension $D - 2$ can be measured from one data set with a specific Reynolds number by applying a box-counting algorithm to the zero-crossings. This method was used by Sreenivasan and his colleagues (see [16] and references therein) who found that the fractal codimension $D - 2$ is indeed well-defined and equal to $2/3$. Another way to measure $D - 2$ is to count the number of zero-crossings in different data sets corresponding to different Reynolds numbers and relate the zero-crossing numbers per unit length to L/η . However, because we do not resolve η in some of our runs, we apply a low-pass filter of wavenumber $2\pi/l_c$ in order to remove the poorly resolved dissipation range and the high-frequency electronic noise of our measuring device. The filter wavenumber is in fact equal to $2\pi/\eta$ for the smallest Reynolds numbers and turns out to be closer to the Taylor microscale wavenumber in most cases. This is the method we have applied here and we have found that the zero-crossing number per unit length is proportional to $(L/l_c)^{2/3}$ which implies $D - 2 = 2/3$. From $D_s = 3(D - 2)$ we deduce $D_s = 2$ in support of our DNS findings.

To explore the relation between the turbulent diffusion of fluid element pairs and the fractal structure of straining stagnation points in the flow, i.e. between (1) and (2), we need to find ways to modify the spatial distribution of straining stagnation points and monitor the changes in turbulent pair diffusion brought about by such modifications. Such a study cannot be carried out with current DNS and laboratory experiments of homogeneous isotropic incompressible turbulence because the spatial distribution of straining stagnation points is determined by the Navier-Stokes dynamics and cannot be tampered with. KS, however, offers the flexibility to choose the energy spectrum at will and thereby modify, as we show below, the fractal structure of the set of straining stagnation points. An additional advantage of KS is that the Lagrangian pair diffusion statistics it produces compare well with DNS results when the energy spectrum chosen is that of the DNS turbulence [8]. KS also successfully generates [12] all the pair diffusion results of the laboratory experiment of [13].

KS uses turbulent-like velocity fields of the form

$$\mathbf{u} = \sum_{n=1}^{N_k} \mathbf{A}_n \wedge \hat{\mathbf{k}}_n \cos(\mathbf{k}_n \cdot \mathbf{x} + \omega_n t) + \mathbf{B}_n \wedge \hat{\mathbf{k}}_n \sin(\mathbf{k}_n \cdot \mathbf{x} + \omega_n t) \quad (3)$$

where N_k (typically of order 100) is the number of modes, $\hat{\mathbf{k}}_n$ is a random unit vector ($\mathbf{k}_n = k_n \hat{\mathbf{k}}_n$), and the directions and orientations of \mathbf{A}_n and \mathbf{B}_n are chosen randomly under the constraint that they be normal to $\hat{\mathbf{k}}_n$ and uncorrelated with the directions and orientations of all other wave modes. Note that the velocity field (3) is

incompressible by construction, and also statistically stationary, homogeneous and isotropic as shown by [9] and [11]. The amplitudes A_n and B_n of the vectors \mathbf{A}_n and \mathbf{B}_n are determined by $A_n^2 = B_n^2 = \frac{2}{3} E(k_n) \Delta k_n$ where $E(k)$ is the energy spectrum prescribed to be of the form

$$E(k) = \frac{u'^2(p-1)}{2(L/2\pi)^{p-1}} k^{-p} \quad (4)$$

in the range $2\pi/L_1 = k_1 \leq k \leq k_{N_k} = 2\pi/\eta$, and $E(k)=0$ otherwise; u' is the rms velocity of the KS turbulent-like flow; $\Delta k_n = (k_{n+1} - k_{n-1})/2$ for $2 \leq n \leq N_k - 1$, $\Delta k_1 = (k_2 - k_1)/2$ and $\Delta k_{N_k} = (k_{N_k} - k_{N_k-1})/2$. The distribution of wavenumbers is geometric (see Flohr & Vassilicos 2000), specifically $k_n = k_1 a^{n-1}$ with a constant a determined by $L/\eta = a^{N_k-1}$. The frequencies ω_n in (3) are proportional to the eddy-turnover frequency of mode n , i.e. $\omega_n = 0.5 \sqrt{k_n^3 E(k_n)}$.

We have varied the power p of the energy spectrum in the range $1 < p < 3$ without changing u' . For a given value of p , we calculate the number of stagnation points by the Newton-Raphson method for different values of L/η . It turns out, as in the case of DNS turbulence, that the vast majority of stagnation points are straining stagnation points irrespective of the values of p and L/η (see figure 1). We also find that, when $p = 5/3$, n_s is proportional to $(L/\eta)^{D_s}$ with $D_s = 2$ (see figure 2), in agreement with our DNS and wind tunnel results. The relation (2) is found to hold for all values of p between 1 and 3 in instantaneous realisations of our KS field and in fact D_s decreases towards 0 as p increases towards 3. Varying p in KS is therefore a good way to tamper with the fractal structure of the set of straining stagnation points in the turbulent-like flow and study what the effects of this tampering are on turbulent pair-diffusion.

We have calculated the time-dependence of the mean square distance between pairs of fluid elements in KS turbulent-like flows for different values of p between 1 and 2 and have found that (1) is valid in the inertial range with

$$\gamma = 6/D_s \quad (5)$$

(see figure 3), and that the Richardson constant G is an increasing function of D_s . For values of p between 2 and 3 we do not find evidence of a well-defined power law (1) and of course nothing like (5). The reason, which we believe lies behind this pair-diffusion behaviour, is that for p between 2 and 3 the power spectrum $k^2 E(k)$ of the strain rate field is concentrated at the smaller wavenumbers when $p > 2$ but increases with wavenumber when $p < 2$. The energy spectrum of a homogeneous and isotropic gaussian velocity field such as (3) for large enough N_k is related to the fractal dimension of zero-crossing surfaces by Orey's relation $p + 2(D - 2) = 3$ (see [17]) which implies $p + 2D_s/3 = 3$. [11] have shown that, as a consequence of pair-diffusion locality, $\gamma = 4/(3 - p)$. Hence, (5) is effectively a consequence of velocity field gaussianity and pair-diffusion locality.

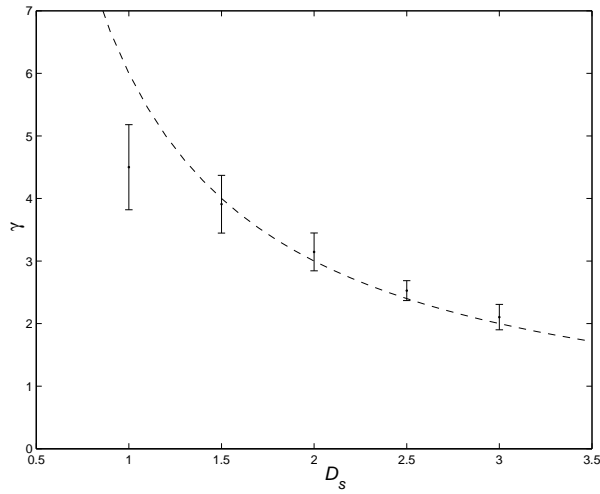


FIG. 3: Relation between Richardson's pair diffusion exponent γ and the fractal dimension of stagnation points D_s . The values of γ are obtained from linear fits of the time dependence of $\overline{\Delta^2}$ (in log-log scale) over the interval where $(3\eta)^2 < \overline{\Delta^2} < (L/3)^2$. The length of the error bars is twice the r.m.s. of γ within that interval. In these KS calculations, $N_k = 40$, $L/\eta = 10^3$ and the initial separation is $\eta/2$ for 2000 different particle pairs. The dashed line shows (5) for comparison.

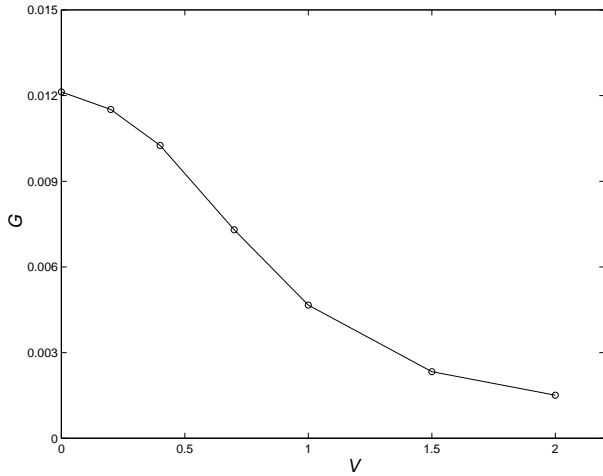


FIG. 4: Richardson constant G versus flow average velocity V using the parameters of the simulations as in figure 3.

Another way to modify the straining flow structure of the KS turbulence is by adding a constant (time and space independent) velocity vector \mathbf{V} to the KS velocity field (3). The KS velocity field defined in (3) is a mean-zero velocity field and the addition of \mathbf{V} amounts to a superposition of a constant mean flow. The aim is to look for stagnation points of $\mathbf{u} + \mathbf{V}$ and monitor the changes in the straining stagnation point structure caused by changes in $V = |\mathbf{V}|$ whilst keeping p constant. Our first observation is that (1) remains valid with the

same value of D_s but C_s decreases with V (see figure 2). By releasing fluid element pairs in the velocity field $\mathbf{u} + \mathbf{V}$ we can study modifications to the Richardson law (1) caused by the mean flow velocity \mathbf{V} . The effects on (1) parallel those on (2): the exponent γ remains well-defined in the same range of times and is independent of V but the Richardson constant G decreases with increasing V (figure 4). The addition of a constant mean flow velocity leaves the scaling exponents γ and D_s of the Richardson law and of the fractal straining stagnation point structure intact, but reduces the overall number of straining stagnation points per unit volume and also the overall extent of turbulent pair diffusion. In view of this conclusion and also of relation (5) there is clearly a correlation between Richardson pair diffusion and the fractal spatial distribution of straining stagnation points in the turbulent-like flow. Such a correlation hints at a certain persistence in time of the streamline structure of the flow which causes pairs to separate when they meet straining stagnation points. This is consistent with our results that G is an increasing function of D_s and of $1/V$, i.e. an increasing function of the number of straining stagnation points in both cases.

We are grateful to Mr. Daniel Polo and Dr. Peter Flohr for help with laboratory and DNS data respectively. JCV acknowledges support from the Royal Society of London and the Hong Kong Research Grant Council (project number HKUST6121/00P).

* Electronic address: davila@eurus2.us.es

- [1] J.M. Otino (1989), "The kinematics of mixing: stretching, chaos, and transport", Cambridge University Press.
- [2] A. Obukhov (1941), *Bull. Acad. Sci. U.S.S.R., Geog. & Geophys., Moscow* **5**, 453.
- [3] G.K. Batchelor (1950), *Q.J.R. Meteorol. Soc.* **76** 133.
- [4] S. Ott & J. Mann (2000), *J. Fluid Mech.* **422**, 207-223.
- [5] G. Pedrizzetti & E.A. Novikov (1994), *J. Fluid Mech.* **280**, 69.
- [6] B.M.O. Heppel (1997), *J. Fluid Mech.* **357**, 167.
- [7] P.K. Yeung (1994), *Phys. Fluids* **6**, 3416.
- [8] N.A. Malik & J.C. Vassilicos (1999), *Phys. Fluids* **11**, 1572.
- [9] J.C.H. Fung, J.C.R. Hunt, N.A. Malik, and R.J. Perkins (1992), *J. Fluid Mech.* **236**, 281.
- [10] F.W. Elliott & A.J. Majda (1996), *Phys. Fluids* **8**, 1052.
- [11] J.C.H. Fung & J.C. Vassilicos (1998), *Phys. Rev. E* **57**, 1677-1690.
- [12] F. Nicolleau & C. Vassilicos (2002), *Phys. Rev. Lett.* (submitted). Also <http://arXiv.org/abs/nlin.CD/0205003>.
- [13] M.C. Jullien, J. Paret & P. Tabeling (1999), *Phys. Rev. Lett.* **82**, 2872.
- [14] W.H. Press, S.A. Teutolsky, W.T. Vetterling & B.P. Flannery (1992), "Numerical Recipes in C", Cambridge University Press.
- [15] Falconer (1990), "Fractal geometry. Mathematical Foundations and Applications", Wiley & Sons, Chichester.

- [16] Sreenivasan (1991), *Ann. Rev. Fluid Mech.* **57**, 539-600. **15**, 249.
- [17] Orey (1970), *Z. Wahrscheinlichkeitstheorie verw. Geb.*